Optimization of physico-chemical and membrane filtration processes to remove high molecular weight polymers from produced water in enhanced oil recovery operations

Optimization of physico-chemical and membrane filtration processes to remove high molecular weight polymers from produced water in enhanced oil recovery operations

Francesco Ricceri,[1,2†] Giulio Farinelli,[1†] Mattia Giagnorio,[1] Aurora Zamboi,[1] Alberto Tiraferri[1,2]*

1: Department of Environment, Land and Infrastructure Engineering, Politecnico di Torino, Corso Duca degli Abruzzi, 24 – 10129 Torino (Italy)

2: CleanWaterCenter@PoliTo, Corso Duca degli Abruzzi, 24 – 10129 Torino (Italy), web: http://cleanwater.polito.it/

[†] *These authors contributed equally*

[*] Corresponding Author.

Email: alberto.tiraferri@polito.it; Tel: +39 011-090-7628, Fax: +39 011-090-7611.

Abstract

Polymer flooding is an enhanced oil recovery technique to extract the large portion of leftover subsurface oil following conventional extraction methods. In the flooding process, a long-chain polymer, such as partially hydrolyzed polyacrylamide (HPAM), is added to the displacing fluid to increase the mobility and extraction of the oil phase. Nevertheless, the challenge of managing produced water from polymer flooding operations is high because residual HPAM results in significantly high viscosity and organic content in the stream. Commonly used methods for produced water treatment, such as gravity settling and flotation, cannot be applied to obtain a purified stream efficiently, while innovative techniques are not yet feasible in practical operations. In this work, a simple method of polymer precipitation prompted by divalent ions is evaluated, optimized, and compared to membrane ultrafiltration. The physico-chemical properties of the HPAM are investigated and polymer precipitation tests are conducted by varying the main operational parameters, including pH, salinity, temperature, calcium and/or magnesium concentration, and polymer concentration. Response surface developed by central composite design method is used to optimize the process and identify the correct dosage of divalent cations coagulants and pH, the two main factors promoting HPAM separation. The removal of HPAM is well-described and maximized (>85%) by the model, which is also validated on three synthetic samples representing real wastewaters from polymer flooding applications. Optimized ultrafiltration, using ceramic membranes with surface pore size of 15 kDa, also shows the ability to remove HPAM effectively from water, but the precipitation method seems to be more versatile and easier to apply. The two processes, precipitation and ultrafiltration, may potentially be used in sequence as they complement each other in several ways.

Keywords: Polymer flooding; Produced water; HPAM; Precipitation; Response surface methodology; Ultrafiltration.

1. Introduction

Enhanced oil recovery (EOR) refers to the process of producing liquid hydrocarbons by increasing the mobility of the displacing phase (Alvarado and Manrique, 2010; Green and Willhite, 2018). Conventional recovery methods, such as water and gas injection, can extract about one third of the initial oil in the formation, and the remaining resource is a large and attractive target for EOR methods (Green and Willhite, 2018; Thomas, 2008). Among the various EOR techniques, polymer flooding (PF) represents an affirmed low-cost method to improve the oil extraction efficiency. In PF, water-based solutions of high molecular weight polymers are injected into the formation to improve the mobility of the oil resource, principally by enhancing the viscosity of the injected fluid (Duan et al., 2014; Manichand et al., 2013; Rostami et al., 2018; Wang et al., 2011a). In particular, partially hydrolyzed polyacrylamide (HPAM) is the most used polymer in PF due to its relatively low cost and high efficiency (Gao et al., 2014; Morel et al., 2012).

In the extraction industry, one of the major environmental problems related to oil recovery is the generation of produced water (PW), representing the largest waste stream of this industrial activity. PW is generally a highly complex matrix, rich in salts and organic compounds, such as dispersed oils toxic dissolved substances (e.g., phenols) (Deng et al., 2002; Gregory et al., 2011; Maguire-Boyle and Barron, 2014; Olsson et al., 2013). When HPAM is used for PF, the PW also contains a considerable amount of the residual polymer, resulting in a more stable oil–water emulsion.(Taylor et al., 2007) and causing levels of viscosity that are too high to safely discharging or efficiently reinjecting the water in reuse schemes (Hoek et al., 2021; Lopes and Silveira, 2014). For those reasons, commonly used method for PW treatment, such as gravity settling and flotation (Thoma et al., 1999), demulsification (Janiyani et al., 1994; Lee and Lee, 2000), or conventional membrane separation (Bilstad and Espedal, 1996; Cheryan and Rajagopalan, 1998; Lipp et al., 1988; Visvanathan et al., 2000; Zhang et al., 2010) may be

inefficient for streams deriving from polymer flooding applications. From this prospective, considerably more efforts should be devoted to developing low-cost and efficient methods able to separate the polymer from the stream in the light of water reuse schemes and stringent discharge regulations.

Among relevant works developed in the last few decades, Deng *et al.* reported a strategy involving a crossflow oil–water separator to remove HPAM from PW (Deng et al., 2002). However, this separation process is associated with high capital and maintenance costs and has limited applicability, i.e., it is only efficient at low polymer concentrations. Chemical and biological processes were also studied as pre-treatments of polymer flooding PW, and interesting results were reported in the literature (Dickhout et al., 2017; Thoma et al., 1999; Zhao et al., 2008). In 2015, Yongrui *et al.* tested Fenton oxidation combined with biological processes to treat polymer flooding PW (Yongrui et al., 2015). The use of photocatalysis (TiO_2) was also investigated to degrade HPAM (Al-Sabahi et al., 2018; Han et al., 2020). However, a major risk of an oxidative method is the potential generation of toxic by-products, which would require at least one additional degradation or separation step to ensure the effluent safety (Munoz et al., 2011; Perez-Moya et al., 2007). Moreover, chemical/biological degradation systems may result in high capital and operational costs, especially related to sludge management (Amudha et al., 2016; Zhou et al., 2018). Literature reports suggest that ceramic membranes may potentially be applied for PW treatment from PF operations thanks to their high stability in harsh environments (Dickhout et al., 2017; Ebrahimi et al., 2010; Zhang et al., 2013). However, only few studies report the applicability of these membranes in the presence of significant polymer concentrations in solution (Fakhru'l-Razi et al., 2010). A study performed by Wang *et al.* (Wang et al., 2011b) demonstrated that hydrolyzed PAM had a more significant impact on the membrane critical flux than did the oil and the suspended solids in the stream. However, previous studies mainly focused on fouling phenomena rather than process

performance and optimization in the range of realistic conditions related to PF applications. In summary, given the emerging use of PF application and the limitations in produced water treatment, there is an increasing and urgent need to find appropriate treatment techniques for such complex and uniquely viscous streams.

As reported in the literature, HPAM behavior is particularly sensitive to salinity (Al-Hamairi and AlAmeri, 2020; Lee et al.; Samanta et al., 2010b). It is widely accepted that precipitation during EOR applications and consequent process impairment is often the result of the interaction between divalent cations and the carboxylate groups present within the hydrolyzed polymer. More in detail, the interaction of the carboxylate groups of HPAM with divalent cations may induce the coagulation and the consequent precipitation of the polymer at a certain ionic concentrations, specifically, at the so-called cloud point (Bae et al., 1991). This phenomenon, and thus the HPAM coagulation mechanisms, are also functions of temperature and pH (Cao et al., 2011; Moradi-Araghi and Doe, 1987). For this reason, PF is not usually applied when oilfield total dissolved solids (TDS) concentrations are above 20 g/L and the temperature is higher than 70 °C, above which the flooding solution would lose its viscosity and displacing properties (Latil, 1980). However, when the goal is the treatment of a polymer flooding PW, divalent cations, pH, and temperature might represent allies to separate the polymer from the water phase by polymer precipitation.

This work advances a facile physico-chemical polymer separation technique as a low-cost method to remove HPAM from produced water by exploiting common divalent cations, i.e., calcium and magnesium, as added or natural coagulants. To evaluate the best precipitation conditions, the physico-chemical properties of the HPAM and its rheological behavior are discussed along with the best coagulation and precipitation conditions, optimized by means of response surface methodology (RSM) (Giovanni, 1983; Khuri and Mukhopadhyay, 2010) (Righetto et al., 2021a, b). The parameters investigated in this study are the concentrations of

calcium and magnesium, temperature, pH, and salinity. The RSM model is then tested with three diverse synthetic produced waters mimicking the composition of real waters to prove its feasibility in potential real scale scenarios. This work also evaluates the potential applicability of ceramic membranes for the removal of HPAM and discusses their performance against that of the optimized precipitation method. Five ceramic membranes are investigated in the range of microfiltration (MF) and ultrafiltration (UF), under a wide range of HPAM and TDS conditions, aiming at filling the gap in knowledge related to the influence of water chemistry on membrane process performance in PW treatment. Limiting factors of the two processes are thus analyzed with the goal to identify the suitable application ranges for both investigated techniques.

2. Materials and Methods

2.1 Chemicals and membranes

The HPAM was supplied by Yixing Bluwat Chemicals Co., Ltd (China) in the form of powder, while all the salts were purchased from Carlo Erba (Milan, Italy). Five TiO_2-based ceramic membranes were selected for membrane filtration: four UF membranes with molecular weight cut-off ranging from 1 to 150 kDa and one MF membrane with 0.45 µm pore size. Each tubular membrane had an inner diameter of 6 mm and 250 mm length. All the membranes were purchased from TAMI Industries (Montreal, Canada).

2.2 Investigation and optimization of HPAM precipitation

2.2.1 HPAM precipitation tests

The precipitation experiments were performed by varying the concentrations of NaCl, $MgCl_2$, $CaCl_2$, in HPAM solutions of varying polymer concentrations. The other parameters affecting HPAM coagulation, i.e., pH and temperature, were adjusted during each experiment through controlled additions of NaOH and using a water bath, respectively, within specific ranges (7-11 and

25-75 °C). Polymer solutions at different concentrations were prepared from a 1500 ppm stock solution of HPAM dissolved in deionized water with a minimum amount of NaCl (0.25 g/L), essential to lower the solution viscosity, thus improving the deployment of the stock solution. The precipitation tests were performed by immersing a 50 mL beaker containing the HPAM stock solution in a thermostatic bath and by addition of stock salt solutions and NaOH solutions of appropriate amounts to reach the target ionic composition, pH, and HPAM concentration for each test. The precipitation was carried out for only about 1 min under gentle stirring, upon reaching the desired pH. Following this short time, the stirring was stopped, and simple gravity sedimentation was exploited to separate the cleared water from the flocs (see photographic examples in Figure S1 of the Supplementary Material file, SM). The HPAM abatement was determined by measuring the total organic carbon (TOC) of the untreated solution and of the supernatant solution.

2.2.2 Design of experiments and statistical analysis

Design Expert software was used to setup and analyze the response surface methodology (RSM) for precipitation experiments (Bradley, 2007; Carley et al., 2004). Central composite design (CCD) was used to define the number of runs needed to develop an accurate response surface. Temperature, pH, as well as NaCl, HPAM, $MgCl_2$, and $CaCl_2$ concentrations were selected as the six operating factors, while the final HPAM concentration in solution following treatment was the target parameter to be minimized (i.e., the HPAM removal maximized). The limit values of HPAM concentration were selected in order to evaluate the phenomena in the most common range of utilization of HPAM. The Appendix section in the SM provides further details of the applied CCD method and analyses. The selected ranges of investigation for the various factors are reported in **Table 1**, together with the coded experimental values extrapolated by Design Expert software. The CCD method generated 86 total recipes for this study, each with a specific combination of values for the six factors. This procedure allowed weighted probing of the entire multidimensional space. The results of HPAM removal obtained by the precipitation experiments were used as input data to

generate the model according to the best fit. ANOVA was used for the statistical analysis of the results and allowed evaluation of the quality of the model (Miller Jr, 1997).

Table 1. Experimental design of the selected parameters

Factors	Unit	Minimum	Maximum	Coded low	Coded high	Mean
Temperature	(C°)	25	75	34.0	66.0	50
pH		7	12	7.9	11.1	9.5
NaCl	(g/L)	0.25	20	3.8	16.4	10.1
Mg/HPAM	(mM/mg)	0	0.6	0.11	0.49	0.3
Ca/HPAM	(mM/mg)	0	0.6	0.11	0.49	0.3
HPAM	(mg/L)	100	1500	353	1247	800

2.2.3 Synthetic produced water samples mimicking the composition of real streams

Table 2 reports the composition of the three synthetic PWs tested in precipitation experiments aimed at addressing the feasibility of the treatment technology in potential real-case scenarios. The compositions of stream A and B were based on published values related to real PWs resulting from polymer flooding processes (Chen et al., 2015; Torabi et al., 2013). Stream C was instead defined based on real wastewater samples collected by a company, Cannon Oil and Gas Well Service Inc., in one of its field works. For each of the synthetic waters, paraffins were used as representative substances for the oil & grease content, while phenol was added to account for the typical concentration of phenols in PW. TDS comprised sodium chloride, sodium sulfate, sodium bicarbonate, sodium carbonate, magnesium chloride, and calcium chloride, that is, the most abundant ions reported in produced waters (Gregory et al., 2011; Olsson et al., 2013).

Table 2. Composition of the synthetic produced waters investigated in this study mimicking the characteristics of wastewaters: A from Torabi *et al.* (Torabi et al., 2013); B from Chen *et al.* and Wang *et al.* (Chen et al., 2015); C from a real sample (Oman oilfield)

Parameter	Unit	Produced water		
		A	B	C
Paraffins (not dissolved)	(mg/L)	450	Paraffins/water 50% (v/v)	75
HPAM	(mg/L)	500	352	800
Na_2SO_4	(mg/L)	128	128	142
$NaHCO_3$	(mg/L)	428	428	84
Na_2CO_3	(mg/L)	24	24	106
$MgCl_2$	(mg/L)	619	619	95
$CaCl_2$	(mg/L)	766	766	111
NaCl	(mg/L)	7410	7410	4680
Phenol	(mg/L)	75	n. p.	n. p.
Acetate	(mg/L)	n. p.	n. p.	2
Silica	(µL)	n. p.	n. p.	63
Temperature	(°C)	50	65	34
Viscosity	(mPa·s)	34.9	32.0	166

n. p.: not present

2.3 Membrane filtration experiments

Separation experiments through ceramic membranes were performed using a cross-flow lab-scale system. The unit comprises a volumetric pump (Nuert, Pordenone, Italy), a thermally insulated feed tank of 8 L and a lab-scale tubular membrane housing cell (TAMI Industries, Montreal, Canada), consisting of a stainless-steel cylinder of 250 mm length and 10 mm inner diameter. Specifically, a tubular ceramic membrane sample with an active area of 47.1 cm^2 can be allocated within the module. A flowmeter, back-pressure valve, temperature control, and data acquisition system comprising a computer-interfaced balance, were used to monitor the operating parameters and to measure the permeate flux. For each test, 3 L of initial feed solution was used; the feed stream was kept at constant temperature of 50 °C through a thermostatic coil directly immersed in the feed tank. The cross-flow rate of 200 L/h (cross-flow velocity of ~2 m/s) was monitored through a floating disc rotameter and adjusted, along with the operating pressure of 1 bar, by means of a pump inverter and a back-pressure regulator. The permeate flow rate was automatically measured every 3 min.

Preliminary tests were performed for the selection of the most promising membranes to be used for the following high recovery tests. The preliminary tests were performed with a solution of HPAM dissolved in deionized water at a concentration of 100 mg/L, while high recovery tests were performed with synthetic waters composed by varying the concentration of HPAM between 100 to 1500 mg/L (Al-Sabahi et al., 2018; Zhao et al., 2008). During preliminary tests, the permeate stream was recirculated into the feed tank with the aim to keep the same operating polymer concentration during the duration of the experiment, namely, 3 h. The permeate flux trend was monitored and the final steady state flux (J_w) was determined. At the beginning of each preliminary experiment, the water flux of a deionized water feed solution was measured (J_0). Conversely, for high recovery tests, the permeate stream was continuously collected in an external vessel. NaCl was used as representative salt, dissolved in the feed solution at concentrations between 1 to 100 g/L (Chen et al., 2015; Torabi et al., 2013; Zhao et al., 2008), to investigate the effect of the interaction between NaCl and the polymer during filtration. A water recovery target of 80% was set for each experiment. However, some of the filtrations were stopped when the permeate flux reached values below 10 L $m^{-2}h^{-1}$ (LMH), considering such operating conditions unfeasible for real applications. At the end of each filtration, the membrane performance was evaluated through the total flux decline ratio, DRt, calculated as:

Total flux decline ratio (DRt): $\left(1 - {J_p}/{J_{W1}}\right)$ (1)

where J_{w1} and J_p indicate the measured flux at the beginning and the end of the test, respectively (Ricceri et al., 2021). Initial and final permeate TOC values were also analyzed in the recovery tests.

2.4 Analytical and characterization methods

The HPAM concentration in solution was determined with a Shimadzu (Milan, Italian branch) TOC-LCSH FA, E200 (catalytic oxidation on Pt at 680 °C). The calibration was performed using

standards of potassium phthalate, $NaHCO_3/Na_2CO_3$, and KNO_3. The HPAM-TOC correlation was perfectly linear in the investigated range, with an R^2 = 0.99. The HPAM removal rate was calculated as:

$$\text{HPAM removal: } \left(1 - {C_{treated}}/{C_{feed}}\right) \cdot 100 \qquad (2)$$

where C_{treat} and C_{feed} refer to the TOC concentration of the treated sample and the initial feed sample, respectively.

All viscosity measurements were performed with the Anton Paar rheometer, Physica MCR 301 (Brannenburg, Germany). The viscosity was measured under different shear rate conditions, ranging from 1 to 100 s^{-1}, at different polymer concentrations. A shear rate of 10 s^{-1} was selected to investigate the role of NaCl, $MgCl_2$, $CaCl_2$, pH, and temperature. The electrokinetic potential of 100 mg/L HPAM solutions was measured in the pH range between 2 and 10. Here, the role of salinity was investigated by preparing solutions of 100 g/L NaCl, 5 mM $CaCl_2$, or 5 mM $MgCl_2$. The concentrations of different ions were selected for their comparable influence on viscosity. All measurements were performed with a Zetasizer Nano analyzer purchased from Malvern, Italian branch.

3. Results and Discussion

3.1 Physico-chemical and rheological behavior of HPAM

Aqueous HPAM solutions behave as non-Newtonian fluids, characterized by a drop of the viscosity at increasing shear rate (Jung et al., 2013; Lopes and Silveira, 2014); see Figure S2 in the SM. This behavior occurs by virtue of the orientation of the macromolecules along the streamline of flow and the consequent disentanglement of macromolecules (Lewandowska, 2007; Seright et al., 2011). **Figure 1a** shows that the observed viscosity of HPAM solutions increased by increasing the

polymer concentration in water, while an increase in NaCl concentration strongly reduced the viscosity of the fluid. This phenomenon is reasonably related to the charge-shielding ability of NaCl, which thwarts the repulsive forces between the charged carboxyl groups of the polymer (Dautzenberg and Karibyants, 1999). Repulsive forces cause the expansion of the polymer chains and are one of the main causes of the viscous feature of HPAM solutions. As the ionic concentration increases, polymer chains collapse causing a reduction in the degree of entanglement (Al-Hamairi and AlAmeri, 2020; Samanta et al., 2010a). Above 100 mM NaCl, all repulsive forces were screened by salt and no viscosity changes were observed by further increasing NaCl content.

Figure 1b shows the effect of divalent ions ($MgCl_2$, $CaCl_2$) on viscosity. In the absence of NaCl, a dramatic drop of the viscosity was achieved even at low concentrations of divalent ions, i.e., 10 mM. This effect was strongly mitigated by addition of NaCl; as a support to this claim, see the results reported for 1711 mM (100 g/L) NaCl. This behavior suggests that monovalent sodium ions at high concentration would compete with the divalent cations, thus minimizing the coil-globule transition of the polymer chain that would be induced by the latter. Indeed, divalent ions may better suppress the viscosity of HPAM solutions thanks to their higher nominal charge and to their specific interaction/complexation with the carboxylate groups of HPAM (Zhang et al., 2008).

Finally, **Figure 1c** reports the effect of pH and temperature on viscosity, which increased with increasing pH until a value of ~6, namely, the natural pH of the HPAM solution (see titration curve in Figure S4 of the SM). This phenomenon is clearly related to the increase of deprotonated carboxyl groups, hence of electrostatic repulsion, moving toward the pH values at which all the moieties were negatively charged (Samanta et al., 2010a), above which no further increase of the viscosity was observed. On the other hand, the temperature did not visibly affect the viscosity of the HPAM solutions in the investigated range, although some effects were reported in previous reports (Muller, 1981; Zhou et al., 2000). The expected effect associated with the increase of the temperature, which would theoretically reduce the viscosity of the solution, may be mitigated by the

enhancement of the degree of the polymer hydrolysis (i.e., the amount of carboxylate groups).

Zeta potential measurements corroborated the previous discussions (**Figure 1d**), by indicating the expected increase of the negative charge at increasing pH. The presence of ions also strongly reduced the electric potential. Compared to NaCl, divalent ions showed a significantly more effective ability in lowering the potential, whose magnitude was similar at 1171 mM NaCl and 5 mM $CaCl_2$. The substantial difference in ionic strength between these solutions suggests that charge shielding is not the only mechanism at play, but that Mg^{2+} and Ca^{2+} can specifically interact with the deprotonated carboxyl groups of HPAM, thus neutralizing them.

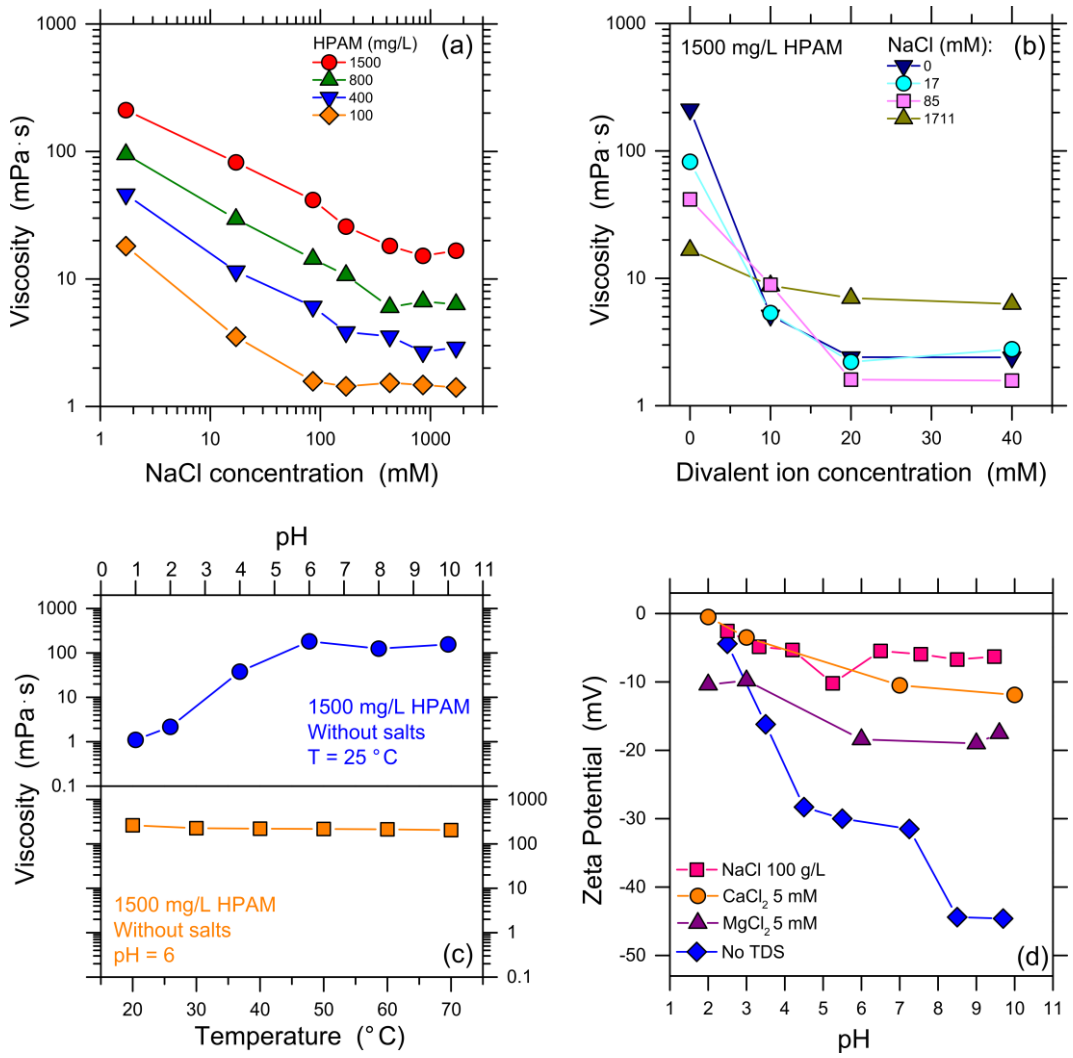

Figure 1. Behavior of HPAM in aqueous solutions. Viscosity measured at a shear rate of 10 s^{-1} as a function of: (a) HPAM and (x axis) NaCl concentrations; (b) NaCl and (x axis) combined divalent

cation concentrations at fixed HPAM concentration of 1500 mg/L; (c) (top) pH and (bottom) temperature in the absence of salinity and at fixed HPAM concentration of 1500 mg/L. In (d), zeta potential values measured as a function of pH in a solution of HPAM 100 mg/L and (pink squares) NaCl 100 g/L, (orange circles) $CaCl_2$ 5 mM, (purple triangles) $MgCl_2$ 5 mM, or (blue diamonds) no salinity. Lines connecting data points are only intended as a guide for the eye. All the experiments where pH was not a factor were performed at the natural pH of a solution of HPAM in water, namely, ~6.

3.2 Modeling and optimization of HPAM removal by precipitation

3.2.1 Results of preliminary precipitation tests and significance of operating factors on HPAM removal

Preliminary tests were performed to assess the influence of different physico-chemical parameters (NaCl, pH, temperature, $MgCl_2$, $CaCl_2$) on HPAM coagulation and precipitation; see Figure S3 in the SM. Results showed that within the investigated range, the influence of $CaCl_2$ and temperature as individual factors on HPAM removal was negligible when tested in a solution of HPAM at 100 mg/L. Interestingly, the effect of the divalent ions on the removal was apparently related to the polymer concentration, with a considerable variation when the divalent ion/HPAM ratio was varied from 0 to 0.6 mM/mg. Results suggest that calcium played an important role in polymer phase separation at large HPAM concentrations (> 800 mg/L). On the other hand, Mg^{2+} was an efficient HPAM coagulant within the entire concentration range, generally resulting in higher polymer phase separation efficiency than calcium. Finally, no significant HPAM precipitation was observed through addition of NaCl within the wide investigated range (Figure S3c of the SM). Based on these preliminary tests, the range of investigation of the various factors influencing HPAM precipitation were selected and used as input for the RSM analysis. Subsequently, the 86 precipitation experiments suggested by the CCD method were performed and the HPAM removal was determined for each test; see **Section 2.2.2** and **Table 1**.

Figure 2 shows diagnostic plots for the removal response of the RSM. As shown in **Figure 2a**, all points fell on a straight line, which implies that residuals had a normal distribution (Pashaei et al., 2020). In **Figure 2b**, all points are included between the externally studentized residuals, justifying the low coefficient of variation (CV) of 17.9 % of the modeling fit. The independence on the order of runs was checked in **Figure 2c**, which shows that the plotted points did not follow a specific pattern (Mason et al., 2003). Moreover, **Figure 2d** shows good agreement between predicted and experimental values (Noordin et al., 2004). In conclusion, the results summarized in **Figure 2** demonstrate ample accordance between the experimental HPAM removal data obtained through precipitation and the relative RSM model.

The significance of each factor in producing HPAM phase separation and sedimentation is related to each respective p-value. As a rule of thumb, a factor is significant, i.e., is correlated to removal, if it presents a p-value <0.1. **Table 3** summarizes the p-values obtained from ANOVA. The pH and the Mg/HPAM ratio were both very significant, consistent with the preliminary tests discussed above. The quadratic cross-correlation terms were also significant, albeit less than pH and Mg dosage. NaCl concentration was not significant and was thus discarded from the model. While temperature, Ca/HPAM ratio, and HPAM concentration were not highly significant (0.1 < p-values < 1), they were however included in the model to respect the hierarchy of the statistical method and to allow the inclusion of all the residuals in the statistical area of the method (Biglarijoo et al., 2016), thus improving the fit. The modeling equation calculated by Design Expert is reported in the SM (Equation S1). This equation allows estimation of the HPAM removal by inserting the values of the five factors included in the model.

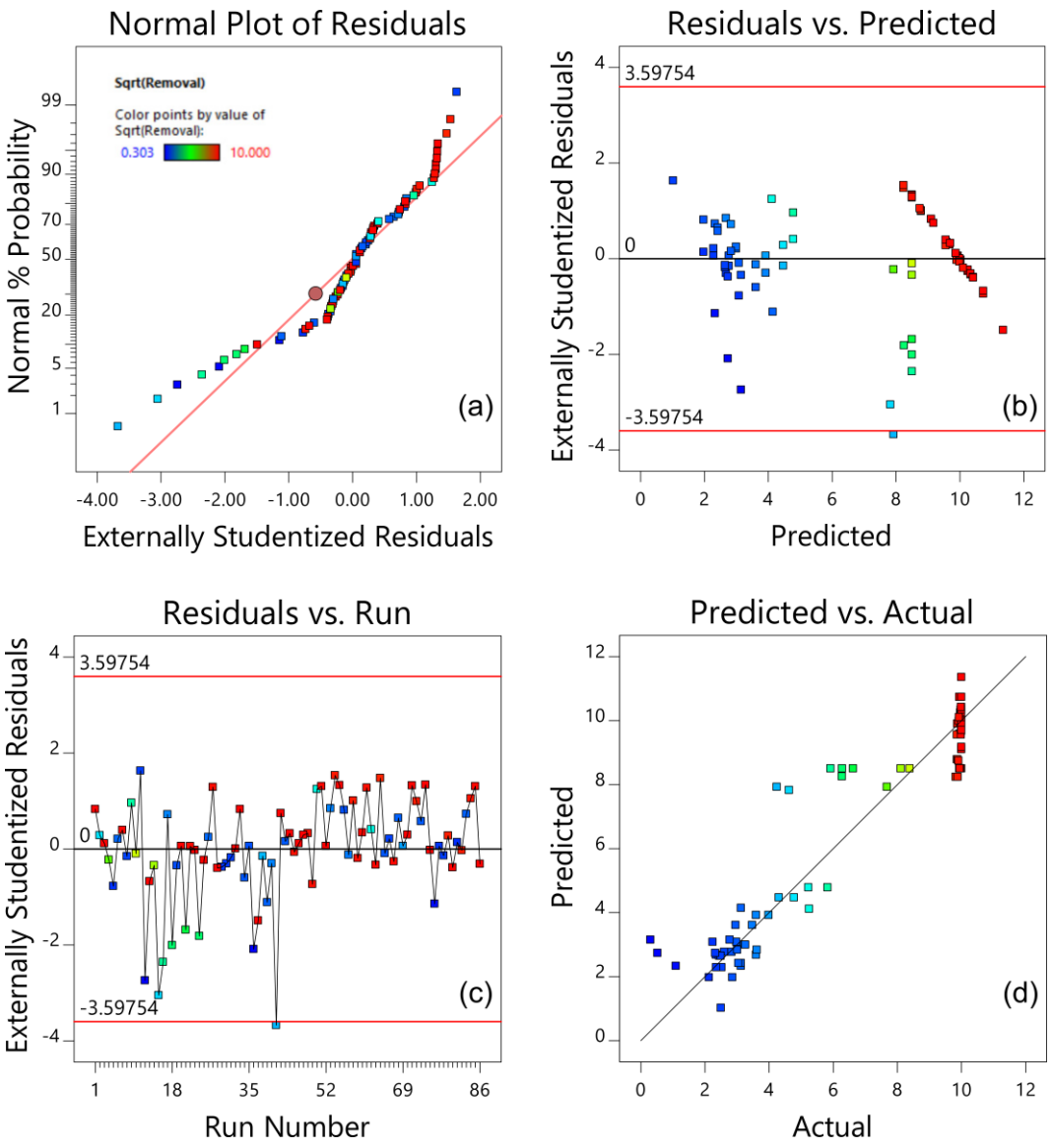

Figure 2. Diagnostic plots for HPAM removal rate response: (a) normal % probability vs. residuals; (b) residuals vs. predicted; (c) residuals vs. test number; (d) predicted vs. actual results. As reported in the legend, colors refer to the square root of the removal values obtained in each of the 86 experiments.

Table 3 Summary of response significance values extracted from the ANOVA table.

Source	Sum of squares	Mean square	F-Value	p-Value
A-Temperature	1.7	1.70	1.25	0.2664
B-pH	751	751	554	< 0.0001
D-Mg/HPAM	12.8	12.8	9.43	0.0030
E-Ca/HPAM	1.14	1.14	0.838	0.3628
F-HPAM	0.0063	0.0063	0.0046	0.9459
BF	6.82	6.82	5.03	0.0279
DF	9.55	9.55	7.04	0.0097
EF	5.85	5.85	4.31	0.0413
B^2	13.85	13.85	10.22	0.0020
E^2	5.11	5.11	3.77	0.0560
F^2	49.57	49.57	36.58	< 0.0001

3.2.2 Single response evaluation

Figure 3 reports an overview of the influence of multiple parameters on HPAM removal process performance, by specifically presenting in each graph the HPAM removal rate as a function of two varying factors (x and y axes), with all the other parameters at their respective mean value (**Table 1**). **Figure 3a** and **3b** present the modeled effect of magnesium and calcium, respectively, on HPAM removal through coagulation and precipitation, at different polymer concentrations. The analysis suggests that the removal efficiency should be higher when HPAM concentration is around 800 mg/L. Moreover, magnesium has projected high efficiency even at low Mg/HPAM ratio. The seemingly unexpected high HPAM removal efficiency at low values of Ca/HPAM is mostly an artefact, due to the concomitant effect of the presence of magnesium in solution in the tests suggested by the CCD method. However, this result allows the reasonable hypothesis of a co-operation of the two cations in the removal of HPAM through phase separation. In particular, the enhancement of the removal efficiency in the presence of Mg^{2+} can be ascribed to the higher ability of carboxyl groups of HPAM to interact with magnesium rather than with calcium, the latter presenting a more localized positive charge (Atouei et al., 2016; Würger et al., 2020).

Generally, the HPAM removal rates predicted by the model linearly increase with increasing pH (**Figure 3c**) and is also higher at mid-concentrations of HPAM. Higher pH would enhance the

ability of HPAM to cross-link in the presence of multivalent cations, hence the ability to form flakes. It would also promote the formation of hydroxides of calcium and magnesium, which are sparingly soluble and act as flocculation enhancers. The strong pH influence on precipitation was confirmed by systematic experimental tests performed in the presence of calcium and magnesium, with results reported in Figure S5 of the SM. Finally, the model predicts the solution temperature to have only minor effects on precipitation (**Figure 3d**).

Overall, the modeling calculations determined from the results of the 86 precipitation experiments were in very good agreement with the physico-chemical and rheological investigation results. The manipulation of the factors influencing the hydrolysis degree of the polymer and the dose of cross-linking agents can effectively be used to control the phase separation and precipitation phenomena. Interestingly, at low and at high HPAM concentrations, the removal rates decreased in the experiments and this phenomenon was correctly captured by the model. At low polymer concentration, there may not be sufficient chains to interact among each other and form sufficiently large flocs. At high concentration, this result may be instead related to the lower diffusivity of salts, hydroxides, or flocs themselves in the medium due to the high viscosity of the solutions. It may also be rationalized with the need of a higher cation concentration than what was investigated in this study to effectively neutralize the higher content of carboxyl groups and induce polymer cross-linking.

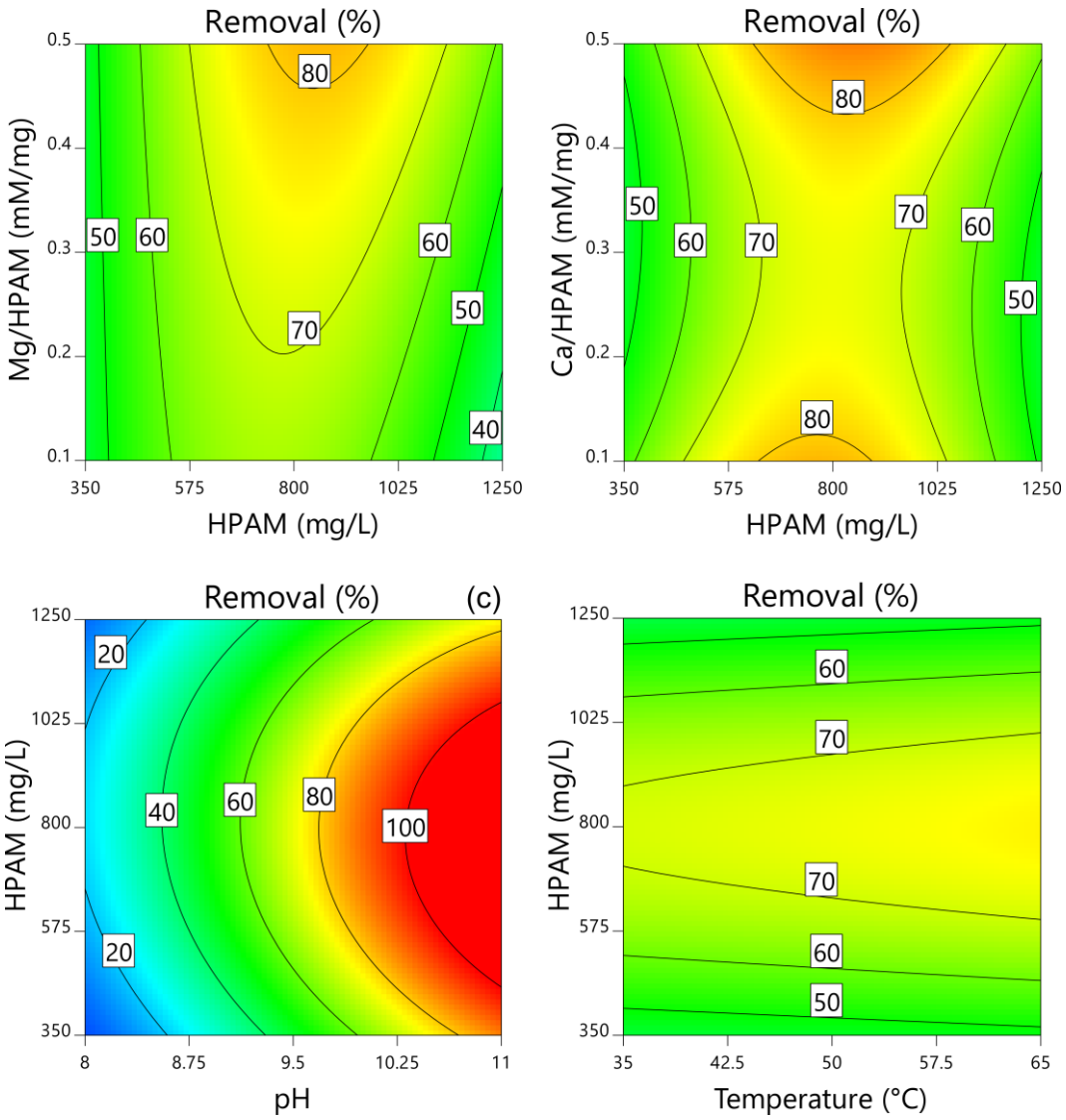

Figure 3. 2D surface response plots for the removal of HPAM as a function of: (a) polymer concentration and magnesium/HPAM concentration ratio; (b) polymer concentration and calcium/HPAM concentration ratio; (c) pH and polymer concentration; and (d) temperature and polymer concentration. HPAM removal rate increases from blue to red. For each graph, the values of the non- plotted parameters are equal to their mean.

3.2.3 HPAM removal in synthetic produced waters mimicking the composition of real waters

An effective treatment is one that minimizes the dosage of coagulation agents, i.e., $MgCl_2$, $CaCl_2$, as well as the chemicals used for pH adjustment, while maximizing HPAM removal. The model developed through the RSM was validated with the three complex streams presented in **Table 2**. In these tests, NaCl concentration, temperature, and HPAM concentration were fixed at the respective realistic values. For each PW, three different scenarios were investigated, with the goal to challenge the model and understand its potential for use with real waters. In scenario 1, the HPAM removal rate was *targeted* to 100%, while the divalent ions concentration and the pH were minimized, the latter up to 11. In scenario 2, the HPAM removal response was *targeted* to values not necessarily as high as 100%, while minimizing the pH (with 10 as the upper limit) and minimizing the divalent ion concentrations. In scenario 3, the HPAM removal was *maximized* within the range 70-100% while the pH was minimized (with 10 as the upper limit) and again minimizing the divalent ions concentrations. The results of the desirability functions are shown in Figure S6, S7, S8 of the SM. As an example, a removal of 99% was predicted by the model in scenario 1 for PW "A" (Figure S6a), with doses of 0.108 mM/mg for both magnesium/HPAM and calcium/HPAM, and a pH value of 10.5. The desirability function was 0.56, the highest among the suggested recipes. On the other hand, when testing the same produced water in scenario 3, the output of the software suggested the use of the same previous ratio of divalent ions/polymer, while lowering the pH to 9.79. This result was obviously obtained at the expense of a lower HPAM removal, which decreased to roughly 77%.

Figure 4 presents the predicted and the experimentally determined removal rates for each of the three produced waters in all the three scenarios. Significantly, the HPAM removal rates measured upon addition of the appropriate reagents as suggested by the model were close to the model prediction (also considering the error) in seven out of the nine cases. The two less consistent cases were related to PW "B" (scenarios 2 and 3), which may be rationalized with the high content of

paraffins (i.e., oil/water 50/50%) that renders the emulsion a complex matrix to treat (Al-Shamrani et al., 2002; Gupta et al., 2017). Notably, the experimental HPAM removal rates were always higher than 85% and, in most cases, higher than the values projected by the model, suggesting that the model is partially conservative in its predictions, and implying the validity of both the model and the precipitation process for a wide range of realistic conditions.

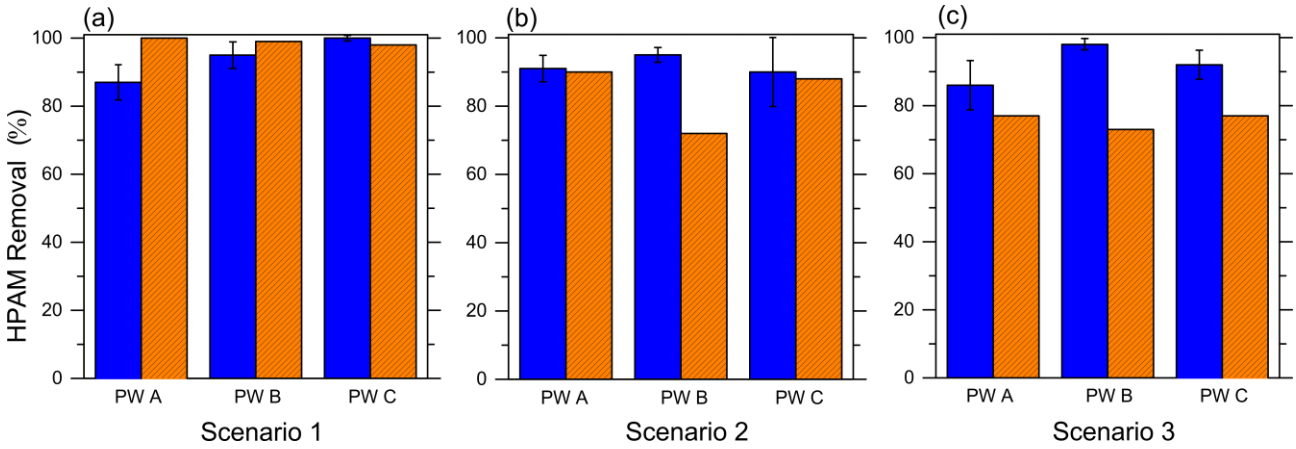

Figure 4. (Blue solid bars) measured and (orange pattern bars) predicted HPAM removal rate for produced waters "A", "B", "C" (Table 2). The error bars for the experimental removal rates represents average and standard deviation values of replicate experiments.

3.4 Productivity of ultrafiltration and removal of HPAM

The results of preliminary membrane filtration tests performed with only HPAM dissolved in water, thus avoiding the presence of other confounders in solution, are reported in Figure S9 of the SM. As expected, the pure water flux before polymer addition (J_0) increased with membrane pore size. After polymer addition (time zero), the permeate flux (J_w) declined instantaneously, suggesting possible rapid clogging of the membrane pores caused by HPAM (Ma et al., 2021). Furthermore, results suggest the existence of a membrane cut-off threshold, above which a critical flux governs the filtration process (Costa and de Pinho, 2005; Yuan and Zydney, 2000): this cut-off threshold was apparently around 15 kDa for this specific application. Indeed, similar permeate flux values were

obtained when treating the HPAM solution by using membranes with larger MWCOs, despite their intrinsic higher permeability (Figure S9b, SM). This interesting result may be ascribed to the quick deposition of HPAM onto the membrane surface and within the surface pores, with the consequent pore clogging (Li et al., 2007; Song, 1998; Wang et al., 2019). On the other hand, membranes with lower MWCO are less subjected to this phenomenon, thanks to the smaller pore size that causes lower permeability but also lower probability of pore clogging and possibly larger turbulence at the membrane/feed stream interface (Mohammadi et al., 2005), which may partially prevent the formation of the cake layer (Vela et al., 2008). Finally, according to the polymer size when dispersed in water (i.e., ~1500 nm, Figure S10 of the SM), membrane filtration always achieved high HPAM rejection (> 92 %).

The results of preliminary tests suggest that membranes with MWCO larger than 15 kDa are not feasible for this specific application. Thus, the high recovery tests were performed by deploying 15 kDa and 5kDa cut-off membranes, with results reported in **Figure 5** at varying feed HPAM concentration and NaCl concentration. While NaCl ranged from 1 to 100 g/L, the investigated polymer concentrations were 100, 800, and 1500 mg/L, reflecting the minimum, medium and maximum values adopted in the HPAM precipitation tests. It is important to note that the presence of divalent ions was not considered in these filtration tests to avoid any possibility of polymer phase separation during the process and to remain conservative in the comparison with the precipitation-based treatment. At 100 mg/L of HPAM, promising results were achieved when filtering a solution with a low NaCl concentration (< 5 g/L) by the 15 kDa membrane, with steady-state permeate flux, J_{w1}, roughly equal to 100 LMH (**Figure 5a**). However, high salinity feed waters were associated with lower performance in terms of permeate flux: J_{w1} decreased to 30 LMH in 5 g/L NaCl solutions and lower than 10 LMH in 100 g/L NaCl, with consequently low permeate recovery achieved in the tests. Recovery experiments suggested that working with a membrane with lower MWCO, namely, 5 kDa, does not entail any substantial benefits. In fact, even in the presence of low

salinity (1 g/L of NaCl), the permeate flux was low and decreased dramatically during filtration, most probably due to the detrimental effects of the polymer concentration increasing within the feed solution during the test, polymer deposition onto the membrane, and the formation of a thick cake layer.

As expected, increasing the HPAM concentration in solution induced a reduction of the permeate flux, also due to higher solution viscosity (**Figure 5b, c**). High HPAM removal rates, similar to what determined during the preliminary tests (92%), were observed even at high polymer concentration. Interestingly, the quality of the permeate stream was not worsened by the increase of salinity, which instead consistently resulted in a more pronounced flux decline during filtration, regardless of the HPAM concentration. This behavior can be more clearly appreciated by evaluating the results summarized in **Figure 5d**, which reports the flux decline ratio (DRt) for the experiments performed with the 15 kDa membrane. This phenomenon may be rationalized with the changes in polymer conformation in the presence of a significant concentration of monovalent ions, also consistent with previous studies (Zhang et al., 2013). At the same time, the solution viscosity did not seem to play a significant role in fouling. This finding is suggested by the decrease of the DRt values with increased polymer concentration, hence viscosity, of the feed solution. This result may be ascribed to: (i) the lower starting flux at higher HPAM concentration; and (ii) the decrease of the NaCl/HPAM ratio, which would entail less overall morphological changes of the polymer chains in solution. To conclude, overall salinity would strongly affect the membrane filtration, while this effect was instead negligible for the HPAM precipitation process.

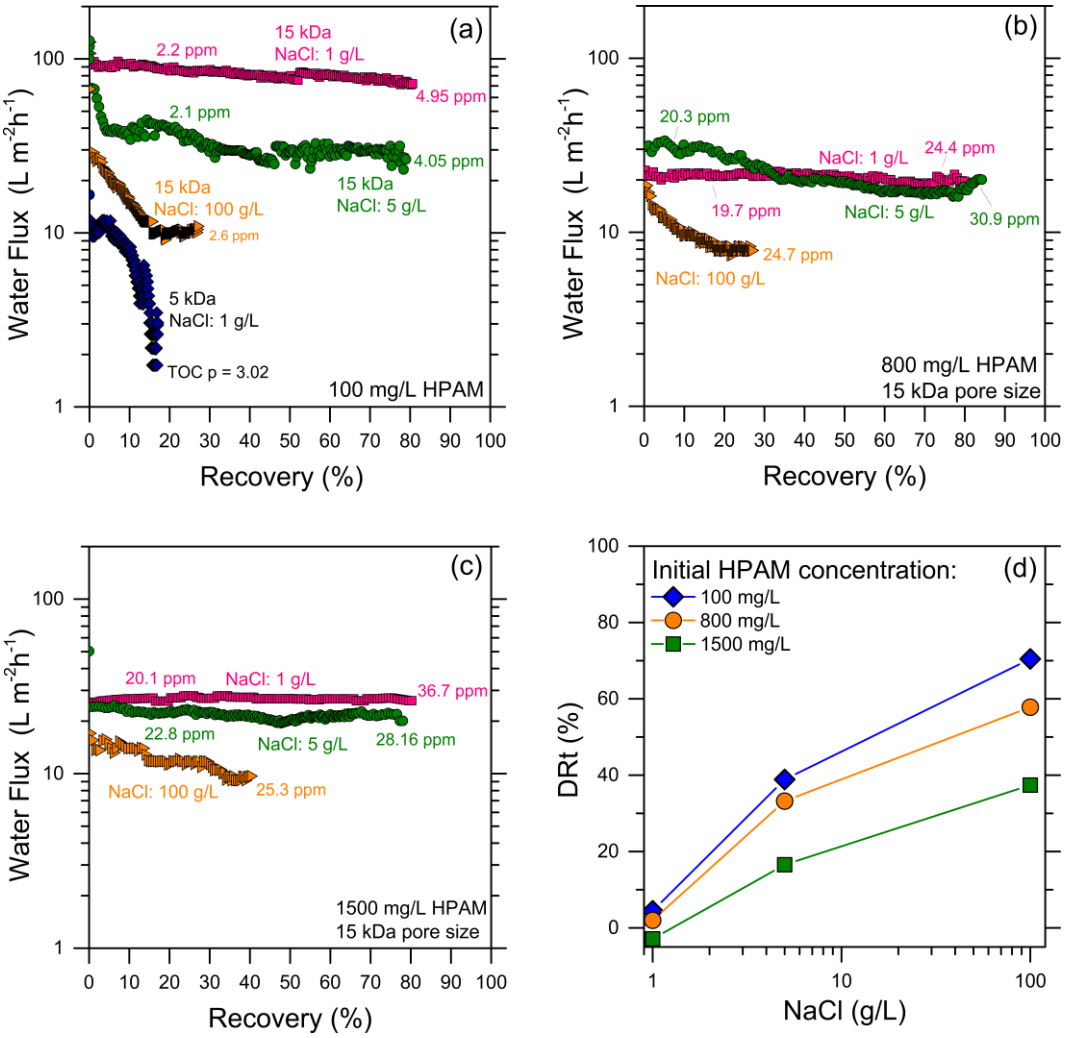

Figure 5. Ultrafiltration experiments with target recovery of 80% performed at 1, 5, and 100 g/L NaCl for different initial polymer concentrations: (a) HPAM concentration of 100 mg/L with 15 kDa and 5 kDa UF membranes; (b) HPAM concentration of 800 mg/L with a 15 kDa UF membrane; (c) HPAM concentration of 1500 mg/L with a 15 kDa UF membrane. In (d), the DRt coefficient for experiments performed with a 15 kDa UF membrane: here, the line connecting the data points is only intended as a guide for the eye.

3.5 Limits and ranges of application of the two investigated HPAM removal techniques

It may be worth discussing the results reported above in the light of the potential integration of the two investigated techniques within PW treatment trains and in relationship to the PW characteristics. UF generally showed high fluxes for relatively low initial concentrations of polymer (100 mg/L) and for low salinity values (1 g/L). The feasible application range of membrane filtration thus appears to be somewhat narrower (i.e., relatively low salinity and organic contents) than that of polymer precipitation, which instead showed a versatile applicability. Indeed, the optimized phase separation and sedimentation process worked efficiently regardless of viscosity and stream salinity. Note that several PWs contain high concentration of divalent cations, which may be exploited as natural coagulants, and the precipitation process would only require a suitable pH increase, in the range 9-11. When the divalent cations concentrations in the PW are low or insufficient to obtain adequate polymer precipitation, these coagulants may be added in the form of salts or hydroxides during treatment. Nevertheless, high dosage of base reagents may be generally required to ensure high HPAM removal rates. It may be interesting to couple the two techniques, thus, to apply precipitation as pre-treatment step for the subsequent ultrafiltration, to abate the concentration of HPAM without necessarily striving to achieve complete HPAM removal, thus minimizing the dosage of coagulation agents and the pH increase. This pre-treatment step would enhance the performance of membrane filtration, provided that the stream is not too salty, and the overall train would guarantee very high HPAM and general TOC removal rates with feasible productivity and with limited needs for chemicals, aimed at the safe management of the final effluent or improved further tertiary treatment, e.g., desalination.

4. Conclusions

Physico-chemical and rheological characterization of HPAM aqueous solutions showed that

Mg^{2+} and Ca^{2+} induced the phase separation of the HPAM polymer at neutral and basic pH values and its precipitation from clean water by simple gravity sedimentation. This mechanism was exploited to remove HPAM and it was optimized through a response surface methodology model. The results of the model allowed identification of the best recipes to achieve HPAM removal (>85%) in complex emulsions mimicking real PW streams. Magnesium dosage and pH were the most influential parameters governing precipitation and may be exploited to remove HPAM from polymer flooding produced water in real application. One of the outcomes of the model is an equation that may be directly applied in field operations to predict and to maximize the HPAM removal from PW by exploiting or adding divalent cations as coagulants and using pH as a trigger parameter. This equation is present in the Supplementary Material.

Moreover, ultrafiltration membranes with 15 kDa cut-off provided the best combination of productivity (100 LMH under 1 bar applied pressure) and HPAM removal (92%) when applied in a surface filtration process. However, ultrafiltration was increasingly less effective in providing a clean permeate with high flux when polymer and salt concentrations were high, conditions that induced more severe fouling. On the other hand, the precipitation method showed high efficiency even for streams of high salinity. Perhaps, the best approach for particularly complex waters and with the goal to obtain high-quality effluents would be to couple precipitation and ultrafiltration within the treatment train, as the two methods appear to complement each other in several ways.

Credit author statement

Francesco Ricceri: Conceptualization, Data curation, Formal analysis, Investigation, Methodology, Visualization, Writing – Original draft, Writing – Review and editing. **Giulio Farinelli**: Conceptualization, Data curation, Formal analysis, Investigation, Methodology, Validation, Writing –Original draft, Writing – Review and editing. **Mattia Giagnorio**:

Conceptualization, Investigation, Validation, Writing – Review and editing. **Aurora Zamboi**: Investigation, Data curation, Writing – Review and editing. **Alberto Tiraferri**: Funding acquisition, Project administration, Resources, Supervision, Visualization, Writing - review & editing.

Acknowledgments

The study was supported by Politecnico di Torino and the CleanWaterCenter@PoliTo (58_DIM20TIRALB; 01_TRIN_CI_CWC).

Declaration of competing interest

The authors declare that they have no known competing financial interests or personal relationships that could have appeared to influence the work reported in this paper.

Appendix A. Supplementary material

Supplementary material for this article can be found online.

References

Al-Hamairi, A., AlAmeri, W., 2020. Development of a novel model to predict HPAM viscosity with the effects of concentration, salinity and divalent content. J. Pet. Explor. Prod. Technol. 10, 1949-1963. https://doi.org/10.1007/s13202-020-00841-4.

Al-Sabahi, J., Bora, T., Claereboudt, M., Al-Abri, M., Dutta, J., 2018. Visible light photocatalytic degradation of HPAM polymer in oil produced water using supported zinc oxide nanorods. Chem. Eng. J. 351, 56-64. https://doi.org/10.1016/j.cej.2018.06.071.

Al-Shamrani, A., James, A., Xiao, H., 2002. Separation of oil from water by dissolved air flotation. Colloid Surf. A 209, 15-26. https://doi.org/10.1016/S0927-7757(02)00208-X.

Alvarado, V., Manrique, E., 2010. Enhanced Oil Recovery: An Update Review. Energies 3, 1529-1575. https://doi.org/10.3390/en3091529.

Amudha, V., Kavitha, S., Fernandez, C., Adishkumar, S., Banu, J.R., 2016. Effect of deflocculation on the efficiency of sludge reduction by Fenton process. Environ. Sci. Pollut. Res. 23, 19281-19291. https://doi.org/10.1007/s11356-016-7118-y.

Atouei, M.T., Rahnemaie, R., Kalanpa, E.G., Davoodi, M.H., 2016. Competitive adsorption of magnesium and calcium with phosphate at the goethite water interface: Kinetics, equilibrium and CD-MUSIC modeling. Chem. Geol. 437, 19-29. https://doi.org/10.1016/j.chemgeo.2016.05.004.

Bae, Y., Lambert, S., Soane, D., Prausnitz, J.M., 1991. Cloud-point curves of polymer solutions from thermooptical measurements. Macromolecules 24, 4403-4407. https://doi.org/10.1021/ma00015a024.

Biglarijoo, N., Mirbagheri, S.A., Ehteshami, M., Ghaznavi, S.M., 2016. Optimization of Fenton process using response surface methodology and analytic hierarchy process for landfill leachate treatment. Process Saf. Environ. 104, 150-160. https://doi.org/10.1016/j.psep.2016.08.019.

Bilstad, T., Espedal, E., 1996. Membrane separation of produced water. Water Sci. Technol 34, 239-246. https://doi.org/10.1016/S0273-1223(96)00810-4.

Bradley, N., 2007. The response surface methodology, Department of Mathematical Sciences. Indiana University South Bend.

Cao, X.C., Guo, H.Y., Li, Y.Y., Chen, M., 2011. The Impact of PH on HPAM Removal from Daqing Oilfield Produced Water Using Clay and Organoclay. Adv. Mat. Res. 239-242, 2210-2213. https://doi.org/10.4028/www.scientific.net/AMR.239-242.2210.

Carley, K.M., Kamneva, N.Y., Reminga, J., 2004. Response surface methodology. Wiley interdisciplinary reviews. Computational statistics. https://doi.org/10.1002/wics.73.

Chen, H.-x., Tang, H.-m., Gong, X.-p., Wang, J.-j., Liu, Y.-g., Duan, M., Zhao, F., 2015. Effect of partially hydrolyzed polyacrylamide on emulsification stability of wastewater produced from polymer flooding. J. Pet. Sci. Eng. 133. https://doi.org/10.1016/j.petrol.2015.06.031.

Cheryan, M., Rajagopalan, N., 1998. Membrane processing of oily streams. Wastewater treatment and waste reduction. J. Membr. Sci. 151, 13-28. https://doi.org/10.1016/S0376-7388(98)00190-2.

Costa, A.R., de Pinho, M.N., 2005. Effect of membrane pore size and solution chemistry on the ultrafiltration of humic substances solutions. J. Membr. Sci. 255, 49-56. https://doi.org/10.1016/j.memsci.2005.01.016.

Dautzenberg, H., Karibyants, N., 1999. Polyelectrolyte complex formation in highly aggregating systems. Effect of salt: response to subsequent addition of NaCl. Macromol. Chem. Phys. 200, 118-125. https://doi.org/10.1002/(SICI)1521-3935(19990101)200:1<118::AID-MACP118>3.0.CO;2-K.

Deng, S., Bai, R., Chen, J.P., Jiang, Z., Yu, G., Zhou, F., Chen, Z., 2002. Produced water from polymer flooding process in crude oil extraction: Characterization and treatment by a novel crossflow oil-water separator. Sep. Purif. Technol. https://doi.org/10.1016/S1383-5866(02)00082-5.

Dickhout, J.M., Moreno, J., Biesheuvel, P.M., Boels, L., Lammertink, R.G.H., Vos, W.M.D., 2017. Produced water treatment by membranes : A review from a colloidal perspective. J. Colloid Interface Sci. 487, 523-534. https://doi.org/10.1016/j.jcis.2016.10.013.

Duan, M., Ma, Y., Fang, S., Shi, P., Zhang, J., Jing, B., 2014. Treatment of wastewater produced from polymer flooding using polyoxyalkylated polyethyleneimine. Sep. Purif. Technol. 133, 160-167. https://doi.org/10.1016/j.seppur.2014.06.058.

Ebrahimi, M., Willershausen, D., Ashaghi, K.S., Engel, L., Placido, L., Mund, P., Bolduan, P., Czermak, P., 2010. Investigations on the use of different ceramic membranes for efficient oil-field produced water treatment. Desalination 250, 991-996. https://doi.org/10.1016/j.desal.2009.09.088.

Fakhru'l-Razi, A., Pendashteh, A., Abidin, Z.Z., Abdullah, L.C., Biak, D.R.A., Madaeni, S.S., 2010. Application of membrane-coupled sequencing batch reactor for oilfield produced water recycle and beneficial re-use. Bioresour. Technol. 101, 6942-6949. https://doi.org/10.1016/j.biortech.2010.04.005.

Gao, C., Shi, J., Zhao, F., 2014. Successful polymer flooding and surfactant-polymer flooding projects at Shengli Oilfield from 1992 to 2012. J. Pet. Explor. Prod. Technol. 4, 1-8. https://doi.org/10.1007/s13202-013-0069-7.

Giovanni, M., 1983. Response surface methodology and product optimization. Food Technol., 41-45.

Green, D.W., Willhite, G.P., 2018. Enhanced oil recovery, 2nd ed. Society of Petroleum Engineers.

Gregory, K.B., Vidic, R.D., Dzombak, D.A., 2011. Water management challenges associated with the production of shale gas by hydraulic fracturing. Elements 7, 181-186. https://doi.org/10.2113/gselements.7.3.181.

Gupta, R.K., Dunderdale, G.J., England, M.W., Hozumi, A., 2017. Oil/water separation techniques: a review of recent progresses and future directions. J. Mater. Chem. A 5, 16025-16058. https://doi.org/10.1039/C7TA02070H.

Han, Y., Zhang, S., Zhang, X., Chen, J., 2020. Electrochemical oxidation of Hydrolyzed Polyacrylamide (HPAM) at Ti/SnO2-Sb2O3/β-PbO2 Anode. Degradation Kinetics and Mechanisms. Int. J. Electrochem. Sci 15, 3382-3399. https://doi.org/10.20964/2020.04.49.

Hoek, E.M., Wang, J., Hancock, T.D., Edalat, A., Bhattacharjee, S., Jassby, D., 2021. Oil & Gas Produced Water Management. Morgan & Claypool publishers.

Janiyani, K., Purohit, H., Shanker, R., Khanna, P., 1994. De-emulsification of oil-in-water emulsions by Bacillus subtilis. World J. Microbiol. Biotechnol. 10, 452-456. https://doi.org/10.1007/BF00144471.

Jung, J.C., Zhang, K., Chon, B.H., Choi, H.J., 2013. Rheology and polymer flooding characteristics of partially hydrolyzed polyacrylamide for enhanced heavy oil recovery. J. Appl. Polym. Sci. 127, 4833-4839. https://doi.org/10.1002/app.38070.

Khuri, A.I., Mukhopadhyay, S., 2010. Response surface methodology. Wiley Interdiscip. Rev. Comput. Stat. 2, 128-149. https://doi.org/10.1002/wics.73.

Latil, M., 1980. Enhanced oil recovery. Editions TECHNIP, Paris, France.

Lee, J.-C., Lee, K.-Y., 2000. Emulsification using environmental compatible emulsifiers and de-emulsification using DC field and immobilized Nocardia amarae. Biotechnol. Lett. 22, 1157-1163. https://doi.org/10.1023/A:1005601525934.

Lee, L.T., Lecourtier, J., Chauveteau, G., Influence of Calcium on Adsorption Properties of Enhanced Oil Recovery Polymers. https://doi.org/10.1021/bk-1989-0396.ch011.

Lewandowska, K., 2007. Comparative studies of rheological properties of polyacrylamide and partially hydrolyzed polyacrylamide solutions. J. Appl. Polym. Sci. 103, 2235-2241. https://doi.org/10.1002/app.25247.

Li, M., Zhao, Y., Zhou, S., Xing, W., Wong, F.-S., 2007. Resistance analysis for ceramic membrane microfiltration of raw soy sauce. J. Membr. Sci. 299, 122-129. https://doi.org/10.1016/j.memsci.2007.04.033.

Lipp, P., Lee, C., Fane, A., Fell, C., 1988. A fundamental study of the ultrafiltration of oil-water emulsions. J. Membr. Sci. 36, 161-177. https://doi.org/10.1016/0376-7388(88)80014-0.

Lopes, L., Silveira, B., 2014. Rheological Evaluation of HPAM fluids for EOR Applications. Int. J. Eng. Technol. https://doi.org/10.1.1.659.6456.

Ma, L., Gutierrez, L., Van Vooren, T., Vanoppen, M., Kazemabad, M., Verliefde, A., Cornelissen, E., 2021. Fate of organic micropollutants in reverse electrodialysis: Influence of membrane fouling and channel clogging. Desalination 512, 115114. https://doi.org/10.1016/j.desal.2021.115114.

Maguire-Boyle, S.J., Barron, A.R., 2014. Organic compounds in produced waters from shale gas wells. Environ. Sci.: Process. Impacts 16, 2237-2248. https://doi.org/10.1039/C4EM00376D.

Manichand, R.N., Moe Soe Let, K.P., Gil, L., Quillien, B., Seright, R.S., 2013. Effective propagation of HPAM solutions through the Tambaredjo reservoir during a polymer flood. SPE Prod. Oper. 28, 358-368. https://doi.org/10.2118/164121-PA.

Mason, R.L., Gunst, R.F., Hess, J.L., 2003. Statistical design and analysis of experiments: with applications to engineering and science, Second edition ed. John Wiley & Sons, New Jersey.

Miller Jr, R.G., 1997. Beyond ANOVA: basics of applied statistics. CRC press, California.

Mohammadi, T., Kohpeyma, A., Sadrzadeh, M., 2005. Mathematical modeling of flux decline in ultrafiltration. Desalination 184, 367-375. https://doi.org/10.1016/j.desal.2005.02.060.

Moradi-Araghi, A., Doe, P.H., 1987. Hydrolysis and Precipitation of Polyacrylamides in Hard Brines At Elevated Temperatures. SPE Reserv. 2, 189-198. https://doi.org/10.2118/13033-PA.

Morel, D.C., Vert, M., Jouenne, S., Gauchet, R., Bouger, Y., 2012. First polymer injection in deep offshore field Angola: recent advances in the Dalia/Camelia field case. J. Pet. Technol. 1, 43-52. https://doi.org/10.2118/135735-PA.

Muller, G., 1981. Thermal stability of high-molecular-weight polyacrylamide aqueous solutions. Polym. Bull. 5, 31-37. https://doi.org/10.1007/BF00255084.

Munoz, M., de Pedro, Z.M., Casas, J.A., Rodriguez, J.J., 2011. Assessment of the generation of chlorinated byproducts upon Fenton-like oxidation of chlorophenols at different conditions. J. Hazard. Mater. 190, 993-1000. https://doi.org/10.1016/j.jhazmat.2011.04.038.

Noordin, M.Y., Venkatesh, V., Sharif, S., Elting, S., Abdullah, A., 2004. Application of response surface methodology in describing the performance of coated carbide tools when turning AISI 1045 steel. J. Mater. Process. Technol. 145, 46-58. https://doi.org/10.1016/S0924-0136(03)00861-6.

Olsson, O., Weichgrebe, D., Rosenwinkel, K.-H., 2013. Hydraulic fracturing wastewater in Germany: composition, treatment, concerns. Environ. Earth Sci. 70, 3895-3906. https://doi.org/10.1007/s12665-013-2535-4.

Pashaei, H., Ghaemi, A., Nasiri, M., Karami, B., 2020. Experimental Modeling and Optimization of CO2 Absorption into Piperazine Solutions Using RSM-CCD Methodology. J. Am. Chem. Soc. 5, 8432-8448. https://doi.org/10.1021/acsomega.9b03363.

Perez-Moya, M., Graells, M., del Valle, L.J., Centelles, E., Mansilla, H.D., 2007. Fenton and photo-Fenton degradation of 2-chlorophenol: Multivariate analysis and toxicity monitoring. Catal. 124, 163-171. https://doi.org/10.1016/j.cattod.2007.03.034.

Ricceri, F., Giagnorio, M., Zodrow, K.R., Tiraferri, A., 2021. Organic fouling in forward osmosis: Governing factors and a direct comparison with membrane filtration driven by hydraulic pressure. J. Membr. Sci. 619, 118759. https://doi.org/10.1016/j.memsci.2020.118759.

Righetto, I., Al-Juboori, R.A., Kaljunen, J.U., Mikola, A., 2021a. Multipurpose treatment of landfill leachate using natural coagulants–Pretreatment for nutrient recovery and removal of heavy metals and micropollutants. J. Environ. Chem. Eng. 9, 105213. https://doi.org/10.1016/j.jece.2021.105213.

Righetto, I., Al-Juboori, R.A., Kaljunen, J.U., Mikola, A., 2021b. Wastewater treatment with starch-based coagulants for nutrient recovery purposes: Testing on lab and pilot scales. J. Environ. Manage. 284, 112021. https://doi.org/10.1016/j.jenvman.2021.112021.

Rostami, A., Kalantari-Meybodi, M., Karimi, M., Tatar, A., Mohammadi, A.H., 2018. Efficient estimation of hydrolyzed polyacrylamide (HPAM) solution viscosity for enhanced oil recovery process by polymer flooding. Oil & Gas Sciences and Technology–Revue d'IFP Energies nouvelles 73, 22. https://doi.org/10.2516/ogst/2018006.

Samanta, A., Bera, A., Ojha, K., Mandal, A., 2010a. Effects of Alkali, Salts, and Surfactant on Rheological Behavior of Partially Hydrolyzed Polyacrylamide Solutions. J. Chem. Eng. Data 55, 4315-4322. https://doi.org/10.1021/je100458a.

Samanta, A., Bera, A., Ojha, K., Mandal, A., 2010b. Effects of Alkali, Salts, and Surfactant on Rheological Behavior of Partially Hydrolyzed Polyacrylamide Solutions †. Journal of Chemical & Engineering Data 55, 4315-4322. https://doi.org/10.1021/je100458a.

Seright, R.S., Fan, T., Wavrik, K., de Carvalho Balaban, R., 2011. New insights into polymer rheology in porous media. Soc. Pet. Eng. J. 16, 35-42. https://doi.org/10.2118/129200-PA.

Song, L., 1998. A new model for the calculation of the limiting flux in ultrafiltration. J. Membr. Sci. 144, 173-185. https://doi.org/10.1016/S0376-7388(98)00057-X.

Taylor, P., Li, M., Xu, M., Lin, M., Wu, Z., Li, M., Xu, M., Lin, M., Wu, Z., 2007. The Effect of HPAM on Crude Oil / Water Interfacial Properties and the Stability of Crude Oil Emulsions The Colloid Surf. A, 37-41. https://doi.org/10.1080/01932690600992829.

Thoma, G.J., Bowen, M.L., Hollensworth, D., 1999. Dissolved air precipitation/solvent sublation for oil-field produced water treatment. Sep. Purif. Technol. 16, 101-107. https://doi.org/10.1016/S1383-5866(98)00115-4.

Thomas, S., 2008. Enhanced Oil Recovery - An Overview. Oil Gas Sci. Technol. 63, 9-19. https://doi.org/10.2516/ogst:2007060.

Torabi, F., Luo, W., Xu, S., 2013. Chemical Degradation of HPAM by Oxidization in Produced Water: Experimental Study. Oil & Gas Science and Technology. https://doi.org/10.2118/163751-MS.

Vela, M.C.V., Blanco, S.Á., García, J.L., Rodríguez, E.B., 2008. Analysis of membrane pore blocking models applied to the ultrafiltration of PEG. Sep. Purif. Technol. 62, 489-498. https://doi.org/10.1016/j.seppur.2008.02.028.

Visvanathan, C., Svenstrup, P., Ariyamethee, P., 2000. Volume reduction of produced water generated from natural gas production process using membrane technology. Water Sci. Technol 41, 117-123. https://doi.org/10.2166/wst.2000.0622.

Wang, B., Wu, T., Li, Y., Sun, D., Yang, M., Gao, Y., Lu, F., Li, X., 2011a. The effects of oil displacement agents on the stability of water produced from ASP (alkaline/surfactant/polymer) flooding. Colloid Surf. A 379, 121-126. https://doi.org/10.1016/j.colsurfa.2010.11.064.

Wang, W., Yue, Q., Guo, K., Bu, F., Shen, X., Gao, B., 2019. Application of Al species in coagulation/ultrafiltration process: Influence of cake layer on membrane fouling. J. Membr. Sci. 572, 161-170. https://doi.org/10.1016/j.memsci.2018.11.014.

Wang, X., Wang, Z., Zhou, Y., Xi, X., Li, W., Yang, L., Wang, X., 2011b. Study of the contribution of the main pollutants in the oilfield polymer-flooding wastewater to the critical flux. Desalination 273, 375-385. https://doi.org/10.1016/j.desal.2011.01.054.

Würger, T., Feiler, C., Vonbun-Feldbauer, G.B., Zheludkevich, M.L., Meißner, R.H., 2020. A first-principles analysis of the charge transfer in magnesium corrosion. Sci. Rep. 10, 1-11. https://doi.org/10.1038/s41598-020-71694-4.

Yongrui, P., Zheng, Z., Bao, M., Li, Y., Zhou, Y., Sang, G., 2015. Treatment of partially hydrolyzed polyacrylamide wastewater by combined Fenton oxidation and anaerobic biological processes. Chem. Eng. J. https://doi.org/10.1016/j.cej.2015.01.034.

Yuan, W., Zydney, A.L., 2000. Humic acid fouling during ultrafiltration. Environ. Sci. Technol. 34, 5043-5050. https://doi.org/10.1021/es0012366.

Zhang, H., Zhong, Z., Xing, W., 2013. Application of ceramic membranes in the treatment of oilfield-produced water: Effects of polyacrylamide and inorganic salts. Desalination 309, 84-90. https://doi.org/10.1016/j.desal.2012.09.012.

Zhang, Q., Zhou, J.-s., Zhai, Y.-a., Liu, F.-q., Gao, G., 2008. Effect of salt solutions on chain structure of partially hydrolyzed polyacrylamide. J. Cent. South Univ. 15, 80-83. https://doi.org/10.1007/s11771−008−319−x.

Zhang, Y., Gao, B., Lu, L., Yue, Q., Wang, Q., Jia, Y., 2010. Treatment of produced water from polymer flooding in oil production by the combined method of hydrolysis acidification-dynamic membrane bioreactor–coagulation process. J. Pet. Sci. Eng. 74, 14-19. https://doi.org/10.1016/j.petrol.2010.08.001.

Zhao, X., Liu, L., Wang, Y., Dai, H., Wang, D., Cai, H., 2008. Influences of partially hydrolyzed polyacrylamide (HPAM) residue on the flocculation behavior of oily wastewater produced from polymer flooding. Sep. Purif. Technol. https://doi.org/10.1016/j.seppur.2008.01.019.

Zhou, G., Willett, J.L., Carriere, C.J., 2000. Temperature dependence of the viscosity of highly starch-filled poly(hydroxy ester ether) biodegradable composites. Rheol. A. 39, 601-606. https://doi.org/10.1007/s003970000096.

Zhou, M., Oturan, M.A., Sires, I., 2018. Electro-Fenton Process. Springer.